International Journal of Pharmaceutics 666 (2024) 124780

Contents lists available at ScienceDirect

International Journal of Pharmaceutics

journal homepage: www.elsevier.com/locate/ijpharm

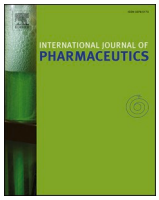

A novel temperature-controlled media milling device to produce drug nanocrystals at the laboratory scale

Elise J. Catlin [a,1], Octavio E. Fandiño [a,1], Lucía Lopez-Vidal [a,b], Martina Sangalli [a], Ryan F. Donnelly [a], Santiago D. Palma [b], Alejandro J. Paredes [a,*]

[a] School of Pharmacy, Queen's University Belfast, Medical Biology Centre, 97 Lisburn Road, Belfast BT9 7BL, UK
[b] Faculty of Chemical Sciences, National University of Córdoba (FCQ-UNC), Haya de la Torre y Medina Allende, X5000XHUA, Córdoba, Argentina

ARTICLE INFO

Keywords:
Media milling
Nanocrystals
Wet bead milling
Nanosuspensions
Top-down
Solid drug nanoparticles

ABSTRACT

Poor aqueous solubility of preexisting and emerging drug molecules is a common issue faced in the field of pharmaceutics. To address this, particle size reduction techniques, including drug micro- and nanonisation have been widely employed. Nanocrystals (NCs), drug particles with particle sizes below 1 μm, offer high drug content, improved dissolution, and long-acting capabilities. Media milling is the most used method to prepare NCs using of-the-shelf machinery, both at the laboratory and industrial scales. However, early NCs development, especially when limited amounts of the active are available, require the use of milligram-scale media milling. This study introduces a novel mini-scale milling device (Mini-mill) that incorporates temperature control through a water-cooled jacket. The device was used to produce NCs of three model hydrophobic drugs, itraconazole, ivermectin and curcumin, with lowest particle sizes of 162.5 ± 0.4 nm, 178 ± 2 nm, and 116.7 ± 0.7 nm, respectively. Precise control of milling temperature was achieved at 15, 45, and 75°C, with drug dependent particle size reduction trends, with no adverse effects on the milling materials or polymorphic changes in the NCs, as confirmed by calorimetric analysis. Finally, a scale-up feasibility study was carried out in a lab-scale NanoDisp®, confirming that the novel Mini-mills are a material-efficient tool for early formulation development, with potential for scale-up to commercial mills.

1. Introduction

Poor water solubility presents a significant challenge to the pharmaceutical industry, as 70 to 90 % of drugs in the development pipeline, and 40 % of drugs on the market exhibit poor water solubility and bioavailability (Ma et al., 2022; Lipinski, 2002). Pharmaceutical companies continue investing in research for new drug molecules with good affinity for the pharmacological target; however, unsatisfactory drug potence due to the low solubility of the compounds often leads to development discontinuation, translating in significant loss of resources and time (McGuckin et al., 2022; Dahan et al., 2016). Particle size reduction is the most universally used strategy to enhance the absorption of poorly soluble actives with micronisation, a technique traditionally achieved *via* milling, allowing the obtention of particles with sizes between 2–10 μm. Work from Liversidge and Cundy, in the early 1990′s, described the production of sub-micrometric drug particles using media milling techniques adapted from the pigments industry (Liversidge and Cundy, 1995). Nanocrystals (NCs) are particles of pure drug with a mean particle size below 1 μm and crystalline properties (Uwe et al., 2008). Unlike conventional polymer and lipid nanoparticles, which require the use of carrier materials, NCs are surrounded by a thin layer of stabiliser, such as surfactants or polymeric stabilisers, to prevent agglomeration. According to the Noyes and Whitney equation, a reduction of particle size increases the dissolution rate by means of increasing the specific surface area, which is critical for Class II drugs in the biopharmaceutical classification system (poor solubility, high permeability) (Noyes and Whitney, 1897; Dizaj et al., 2015; Junyaprasert and Morakul, 2015). NCs can be produced using bottom-up and top-

Abbreviations: CUR, Curcumin; DSC, Differential scanning calorimetry; ITZ, Itraconazole; IVM, Ivermectin; NCs, Nanocrystals; NSs, Nanosuspensions; PEO, Polyethylene oxide; POL 188, Poloxamer 188; PPO, Polypropylene oxide; PDI, Polydispersity index; PVA, Polyvinyl alcohol; TGA, Thermal gravimetric analysis; SEM, Scanning electron microscopy; SERL, Solvent resistant electrode.

* Corresponding author at: School of Pharmacy, Queen's University Belfast, Medical Biology Centre, 97 Lisburn Road, Belfast BT9 7BL, UK.
E-mail address: a.paredes@qub.ac.uk (A.J. Paredes).

[1] These authors contributed equally to this work.

https://doi.org/10.1016/j.ijpharm.2024.124780
Received 30 August 2024; Received in revised form 27 September 2024; Accepted 27 September 2024
Available online 28 September 2024

down techniques, leading to NCs suspensions, also known as nano-suspensions (NSs), with further water removal forming powdered NCs. NCs have made a significant clinical impact, with > 20 products on the market, including the recently approved long-acting injectable antiretroviral Cabenuva®, which marked and important milestone for the field.

Top-down techniques are the most employed, both in academic and industrial laboratories, with the primary benefit of achieving high drug loadings, while using water as a dispersion media, thus avoiding the use of organic solvents, which are normally required to dissolve the drug before precipitation in bottom-up techniques (Castillo Henríquez et al., 2024). Top-down approaches, on the other hand, require the application of high energy inputs and include techniques such as media milling and high-pressure homogenisation, with the former being the most used approach for the production of the currently marketed NCs products (Malamatari et al., 2018). Media mills consist of a milling chamber where the crude drug is stirred together with an aqueous solution of a stabiliser and the milling media, typically beads of various materials, such as Yttria stabilised zirconia, metal, plastic or glass. Agitation generates collisions, attrition and shear forces which lead to particle breakage and size reduction (Malamatari et al., 2018). One of the major advantages of this process is the possibility to be easily scaled up using of-the-shelf machinery (Müller et al., 2011). Crucially, industrial media mills are equipped with an integrated cooling system enabling precise control of the process temperature *via* an external jacket surrounding the milling chamber through which a cooling fluid circulates (Uwe et al., 2008; Malamatari et al., 2018).

Commercially available mills have processing capacities that require significant amounts of the drug for effective milling, ranging from several grams at the lab scale, to kilograms at the industrial scale (Peltonen, 2018). However, these systems are inconvenient at early stages of drug development when the amount of active is limited, or when working with expensive compounds. Consequently, the production of NCs using simplified, small media milling devices that can be used with milligrams is an interesting target for exploration. Romero *et al*, described the use of a magnetically stirred device with a milling chamber of 2 mL (Romero et al., 2016), whereas work from this group reported the manufacture of NCs using 10 mL vials (Permana et al., 2021; Permana et al., 2020; Bianchi et al., 2022; Zhang et al., 2023; Abbate et al., 2023; Wu et al., 2022). Production of NCs using small-scale wet bead milling within academia has been most beneficial, providing ease and flexibility in terms of formulation optimisation by enabling control over various milling parameters, such as volume of milling media, quantity of drugs and stabilizers, which play a crucial role in the physical properties of the resulting NCs, while producing NCs in a cost, material and energy efficient manner (Chen et al., 2011).

One key difference between the magnetically stirred devices previously described and commercially available mills is the possibility to regulate the temperature of the process, a critical parameter in the milling process, which can affect the rheology of the slurry (drug, surfactant solution and beads) as well as the milling efficiency. Additionally, the heat generated during milling may disrupt the colloidal stability and lead to thermal drug decomposition. Implementation of a cooling jacket may provide superiority in terms of formulation optimisation as this system would allow each parameter to be specifically fine-tuned, per the requirements of the specific API, with the additional benefit of temperature regulation during the milling process. Additionally, employment of a thermally regulated system could be crucial for the extraction of biomolecules from plants, cells and tissues whereby media milling is widely used, and temperature plays a key role with respect to material decomposition.

This work reports the use of an original milling device for the production of drug NCs at the laboratory scale, with the unique feature of permitting temperature control *via* water circulation through a cooling jacket. The manufacture of NCs of three model hydrophobic drugs, itraconazole (ITZ), ivermectin (IVM) and curcumin (CUR) was performed, and manufacturing parameters, such as amount of milling media, milling time and milling temperature is presented. A commercial laboratory scale mill was used to reproduce the milling conditions of the novel mills and demonstrate potential for scale-up.

2. Materials and methodology

2.1. Materials

CUR (CAS RN 458–37-7, molecular weight 368.39), ITZ (CAS RN 84625–61-6 molecular weight 875.11), and IVM (CAS RN 70288–86-7 molecular weight 705.64) were obtained from Tokyo Chemical Industries (United Kingdom). Poloxamer 188 (POL 188) was purchased from BASF Chemical company (Ludwigshafen, Germany). Polyvinyl alcohol (PVA) (9–10 kDa) was purchased from Sigma-Aldrich (Dorset, UK). YTZP Yttria-stabilised zirconia beads with a diameter of 0.1–0.2 mm obtained from Chemco (Guangfu China) were used as the media in the wet media milling process. Ultrapure water was obtained from a water purification system, Elga Purelab DV25, Veolia Water systems (Ireland). All other chemicals were of analytical grade.

2.2. Design and construction of the media milling device

The new media milling device (Mini-mill) were built using glass at the Glass Blowing Shop at Queen's University Belfast, UK. The device consisted of a milling chamber of 12 mL surrounded by a cooling jacket with inlet and outlet connections for water circulation. A screwed neck allowed to close the system hermetically using a screwed plastic cap. The vials were produced using Simax® glass with a composition of 80.3 % SiO_2, 13.0 % B_2O_3, 2.4 % Al_2O_3 and 4.3 % Na_2O+K_2O (Kavalier, Sázava, Czech Republic). Fig. 1 presents illustrations of the device with its dimensions and images of the actual mills.

2.3. CUR, IVM and ITZ bulk powder particle size measurement

A Malvern Mastersizer® 3000 was utilised to measure the initial particle size distribution of the model hydrophobic drugs in the initial coarse powder form, using laser diffraction, prior to size reduction in the Mini-mills. The assay was conducted at room temperature. After dispersion of the particulate matter, a laser beam illuminated the particles, with the intensity of the scattered light collected and analysed to determine the particle size distribution within the sample. In short, 10 mg of the coarse powder of each drug was added to 10 mL of 1 % (w/w) PVA (9–10 kDa) and vortexed, to produce a homogenous suspension. This was further dispersed in a glass beaker containing 500 mL of deionised water. The sample was agitated for 3 mins at 2000 rpm during analysis and sonicated between each measurement cycle for 30 s to confirm an accurate and reproducible dispersion was achieved.

2.4. Preparation of drug NCs using the novel Mini-mills

Three poorly soluble actives were used as model drugs, CUR, ITZ and IVM. NSs of all the drugs were produced using the Mini-mills using the experimental set up described in Fig. 2. To this purpose, 100 mg of the drug were placed in the milling chamber together with 5 mL of 1 % (w/v) POL 188 (selected stabilizer) and 4.5 mL of zirconia beads (0.9:1 vol ratio with the surfactant solution). Additionally, two magnetic bars of 25 x 8 mm (IKAFLON®, Sigma-Aldrich, Dorset, UK) with their magnetic poles aligned were added in the milling chamber, and the system placed on an IKA RCT Basic Magnetic Stirrer (Staufen, Germany) at a rotation speed of 1200 rpm. Each formulation was milled within the temperature-controlled vials at set temperatures of 15 °C, 45 °C and 75 °C with samples taken after 1, 6 and 24 h. Temperature control was achieved by circulation of a coolant fluid (Kryo 30, Lauda Wobser GMBH, Germany) using a Ministat® 125w Pilot one compact cooling bath circulation thermostat (Huber, Offenburg, Germany). After

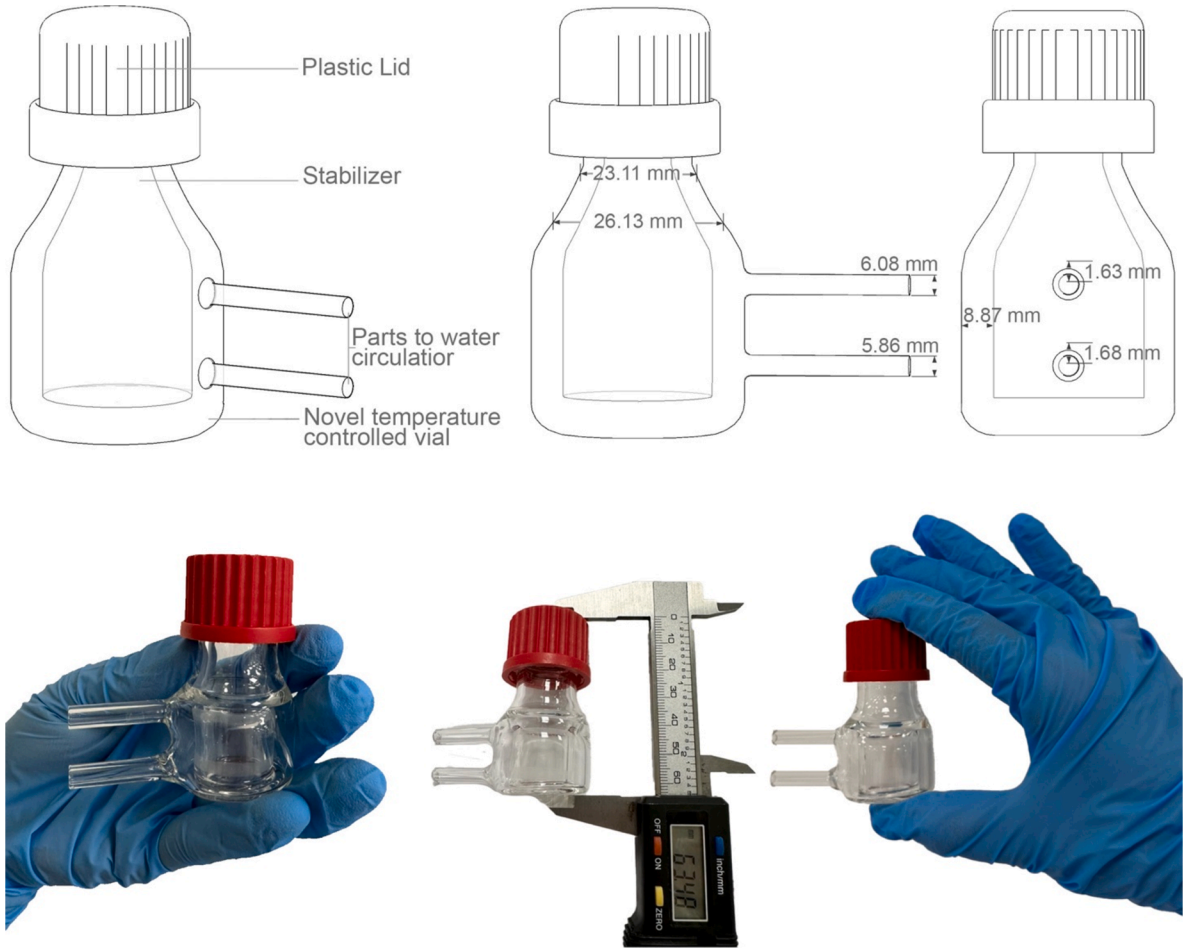

Fig. 1. Images of the novel Mini-mills used for wet bead milling annotated with its dimensions.

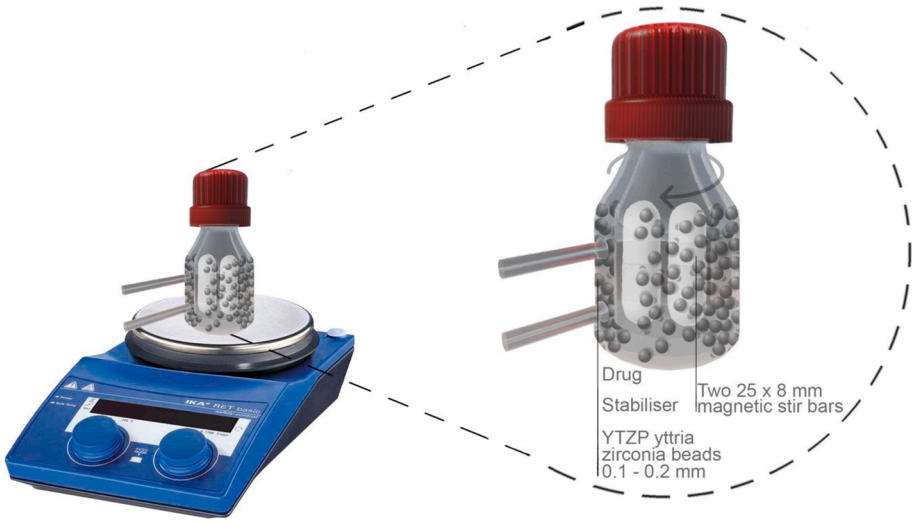

Fig. 2. A schematic representation of the experimental set up employed to produce NCs, *via* wet media milling, using the Mini-mills.

completion of milling at 24 h, the NSs were separated from the milling media and magnets using a nylon 200-mesh sieve (74 μm-pore size) placed over a metal funnel. Following this, the NSs obtained were characterised in terms of particle size, polydispersity index (PDI) and zeta potential as described in the following section 2.6.1. At the end of the process, the resultant NSs were freeze-dried for further analysis in a SP Scientific, Warminster PA, USA freeze-dryer, following a previously reported protocol (Wu et al., 2022).

2.5. Measurement of the vials internal and external temperature

To examine the Mini-mills ability to produce NCs at specified chosen temperatures set *via* the central console display, the internal and external temperature of the vials was measured. Additionally, a control

was employed, whereby the milling experiments were carried out as previously described in the novel Mini-mill device without employment of thermoregulation to determine the change in temperate during the media milling process. The internal temperature of the system was measured using a mercury thermometer directly inside the milling chamber, whereas the external temperature was measured using a UniversalTemp® Infrared Thermometer (Bosch, Gerlingen, Germany). To measure the internal temperature, the milling experiment was paused, and the mercury thermometer immediately placed inside the milling chamber while measurement of the external temperature required the infrared thermometer to be secured in a fixed position by a three fingered clamp. This method was implemented to ensure the angle of measurement across each timepoint remained constant to ensure accurate emissivity, field of view and spot size. All the experiments were carried out in triplicate and the results expressed as means ± SD ($n = 3$).

2.6. Physiochemical characterization of nanosuspensions

2.6.1. Particle size, polydispersity index and zeta potential

A Nanobrook Omni Dynamic Light Scattering Particle Sizer (Brookhaven Instruments, Holtsville, NY, USA) was used to measure the particle size and PDI of each NS, with the particle size measurement provided as the particles' hydrodynamic diameter. Sample preparation consisted of dilution of 20 μL of each sample with 3 mL of ultra-pure water in a plastic cuvette. Additionally, the zeta potential was determined using the same dilution and medium, with phase analysis light scattering which required insertion of a SERL (solvent resistant electrode) plastic probe into the plastic cuvette. All measurements were conducted in triplicate at 25 °C after a 30 s equilibration time and presented as means ± SD (n = 3).

2.6.2. Scanning electron microscopy (SEM) of coarse drugs and nanocrystals

Samples of the coarse drug were placed onto double-sided carbon attached to an aluminium SEM sample holder. For visualisation of the NSs a droplet was pipetted onto the carbon adhesive disk and left to dry at room temperature overnight with all the samples coated with gold prior analysis in a Sigma Scanning Electron Microscope (Zeiss, Oberkochen, Germany). The analysis was carried out with an acceleration voltage of 3–20 kV. For the coarse drugs, a magnification of 300 × was used, with an aperture size of 60.00 μm (width of 381.1 μm). For the obtained NCs, both from the Mini Mill and the Scale-up, images were captured at a magnification of 15,000×, with an aperture size of 60.00 μm and a width of 7.622 μm. Magnifications between 300 × and 15000 × were used to observe the morphology of the particles.

2.6.3. Differential scanning calorimetry (DSC)

DSC was used to assess the crystallinity of the coarse drugs, stabilizer and NCs formed. To this purpose, 5–10 mg of the lyophilised NSs, formulation excipients and coarse drugs were placed in standard hermetic aluminium pans with an empty pan as reference. A Q100 Differential Scanning Calorimeter (TA Instruments, Delaware, USA) was employed with samples heated in nitrogen atmosphere at a stepping rate of 10 °C/min over a temperature range of 25 °C to 350 °C. TA Instruments Universal Analysis 200 Software, version 4.4A (TA Instruments, Elstree, Hertfordshire, UK) was utilised to study and quantify any thermal events.

2.6.4. Thermal gravimetric analysis (TGA)

TGA was used to evaluate the thermal behaviour of the pure drugs, stabilizer and NCs produced. To this purpose, 5–10 mg of each material was carefully weighed into aluminium pans, placed into a platinum sample pan with an attached stirrup and heated from ambient temperature to 500 °C at a heating rate of 10 °C/min in a Thermal Advantage Model Q500 thermogravimetric analyser (TA Instruments, Delaware, USA). During all analysis nitrogen flow rates of 50 mL/min (balance and sample purge gas) were maintained.

2.6.5. pH measurement of CUR, IVM and ITZ nanosuspensions

A HANNA HI-2210–02 benchtop pH meter (Hanna Instruments Ltd., Bedfordshire, UK) was employed to accurately determine the pH of the CUR, IVM and ITZ NSs. The pH meter was calibration using two buffer solutions, one of pH 4.00 ± 0.01 at 25 °C and the other 7.00 ± 0.01 at 25 °C. Each NSs was individually transferred into a 5 mL falcon tube, the pH probe was placed inside the falcon tube and the pH was measured at equilibration of the reading. The probe was removed from the tube and washed with deionized water in between measurements.

2.7. Microscopical analysis of Yttria-stabilised zirconia beads

Scanning electron microscopy images of YTZP yttria zirconia beads were captured using a benchtop TM3030 electronic microscope (Hitachi, Tokyo, Japan) prior to milling and after. This was to allow investigations to be made with respect to the surface morphology and integrity of the beads after exposure to different temperatures during the milling process. The milling media was securely attached to carbon double-sided adhesive disks and placed on an aluminium stage. Images were taken under low vacuum, at a magnification of 400 and at an accelerating voltage of 15 kV.

2.8. Potential scale-up of the Mini-mills

The potential for scale-up of the Mini-mills was assessed using a NanoDisp® media mill (Paredes et al., 2020). To this, the configuration of the system was adjusted to mimic the milling conditions of used with the Mini-mills. The 120 mL-milling chamber was filled with 1.2 g of drug, 60 mL of 1 % w/v POL 188 and 54 mL of Yttria-stabilised zirconia beads. The system was agitated at 1200 rpm and the temperature adjusted to 15 °C. Samples were withdrawn at predetermined intervals for particle size determination and SEM imaging as described in sections 2.5.1 and 2.5.2, respectively.

2.9. Statistical analysis

Microsoft Excel ™ version 16.81 2024 (Microsoft Corporation, Redmond, USA) was used for statistical analysis for calculation of means and S.D. All other statistical analysis was completed using GraphPad Prism® version 9 (GraphPad Software, San Diego, California, USA). The results were presented as means ± SD after measurement in triplicate, in all cases.

3. Results and discussion

3.1. CUR, ITZ and IVM bulk particle size measurement

The particle size distribution of CUR, ITZ and IVM was assessed by individual dispersion of each drug in a 1 % (w/v) PVA (9–10 kDa) solution, as depicted in Fig. 3. The D (Dahan et al., 2016; McGuckin et al., 2022) values, De Brouckere Mean Diameter, representing the average size of the particles with respect to volume are in the micrometre range for CUR, ITZ and IVM at 71.9, 174 and 83.4 μm, respectively. The wide peaks presented in Fig. 3 highlights the varied distribution of non-uniform sized particles, and tendency to aggregate, with ITZ exhibiting a bimodal volume distribution, this therefore indicates the model drugs selected are fit for the intended purpose of significant size reduction and are suitable candidates to manufacture homogenous particles to the nanometre scale.

3.2. Physiochemical characterization of CUR, ITZ and IVM NSs

NCs of the three drugs were prepared, with the mean particle size and PDI of the resultant NSs shown in Fig. 4 alongside the processing

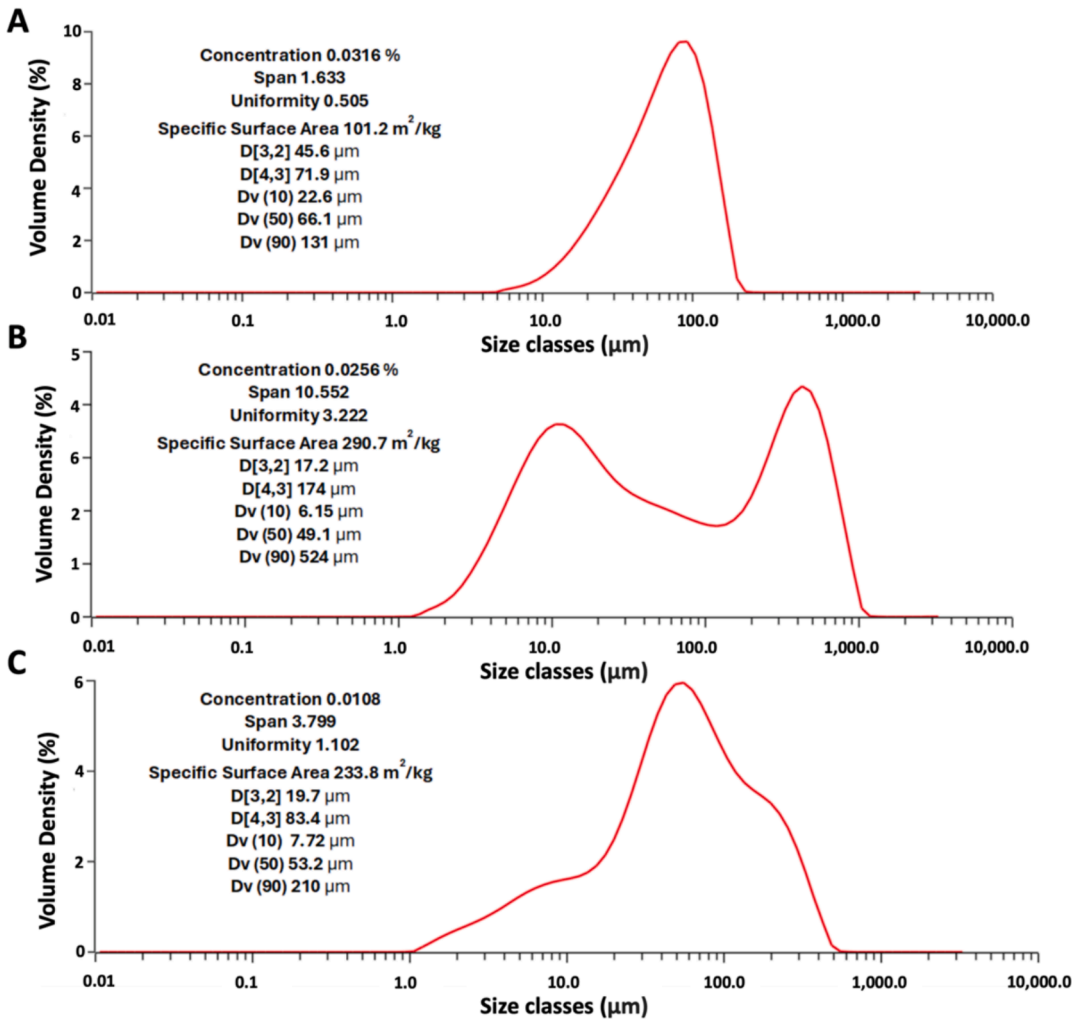

Fig. 3. Particle size distribution graphs of CUR (**A**), ITZ (**B**) and IVM (**C**) dispersions achieved by laser diffraction.

time and milling temperature. After 1 h of milling, it was observed that controlling the temperature had little influence on the particle size of CUR, with slight variation in size amongst all temperatures, indicating temperature control during the early stages of CUR milling temperature does not seem to be a dominant factor in terms of particle size, as highlighted in Fig. 4**A**. However, the opposite was observed with IVM and ITZ, as it is evident 75 °C is the most favourable temperature for IVM milling and 45 °C is the least favourable temperature for ITZ milling, in terms of producing particles of the smallest size. Thus, even after a short period of milling, it is clear manipulation of temperature during milling of certain drugs can be used to alter the size of particles produced. The variation in particle size of CUR after 6 h of milling at different temperatures diminishes even further, suggesting temperature has minimal contribution in determining the particles size of CUR NCs, as depicted in Fig. 4**C**. Similarly, the trends observed for IVM and ITZ at 1 h continues on after 6 h, with higher temperatures yielding smaller particles in the case of IVM and milling ITZ at the elevated temperature of 45 °C produced the largest NCs. After milling ceased at 24 h, 15 °C was shown to be the most appropriate temperature evaluated to fabricate the smallest CUR particles (116.7 ± 0.7 nm), although using higher temperatures still produced particles of a comparable size, as highlighted in Fig. 4**E**. Interestingly, it can be seen that after milling ITZ for an extended period of time, controlling the milling temperature at 45 °C was most favourable with respect to reduction in particle size (162.5 ± 0.4 nm), demonstrating that not only is it beneficial to control the temperature of milling, but also the time at which the milling is controlled for is also significant with regards to particle size. Similarly, controlling the milling for a longer period of time resulted in the production of the smallest IVM-NCs at 45 °C (178 ± 2 nm), with milling at 75 °C closely following despite having a more pronounced importance within a shorter milling period. Clearly, the influence of milling temperature on particle size reduction over time varies considerably among different drugs. While in theory any drug, independently of their physicochemical nature can undergo particle size reduction, to date, specific research where intrinsic crystal hardness and process temperature are factored together in media milling is still necessary. Reports from Prof Keck have commented on drug hardness-dependent particle reduction in media milling, with harder materials predictably leading to larger final particle sizes (Muller and Keck, 2004). In this sense, it could be hypothesised that drugs with higher melting points, and therefore higher intermolecular forces in their crystal lattice, would be more difficult to break. However, other factors need to be weighted when using top-down approaches, including the presence of crystal imperfections, polymorphic forms, solvates/hydrates, and impurities, among others. As per temperature, some reports have delved into heat generation during media milling (Guner et al., 2022; Guner et al., 2022), and NCs production *via* cryo-milling (Niwa et al., 2010); however, little has been reported on the effect of temperature in media milling. Moreover, beyond milling temperature, milling time plays an important role in the final particle size, with most of particle reduction occurring at early stages of the process. This phenomenon is commonly observed in the literature and is related to the gradual reduction of weak points and cracks in the drugs crystal

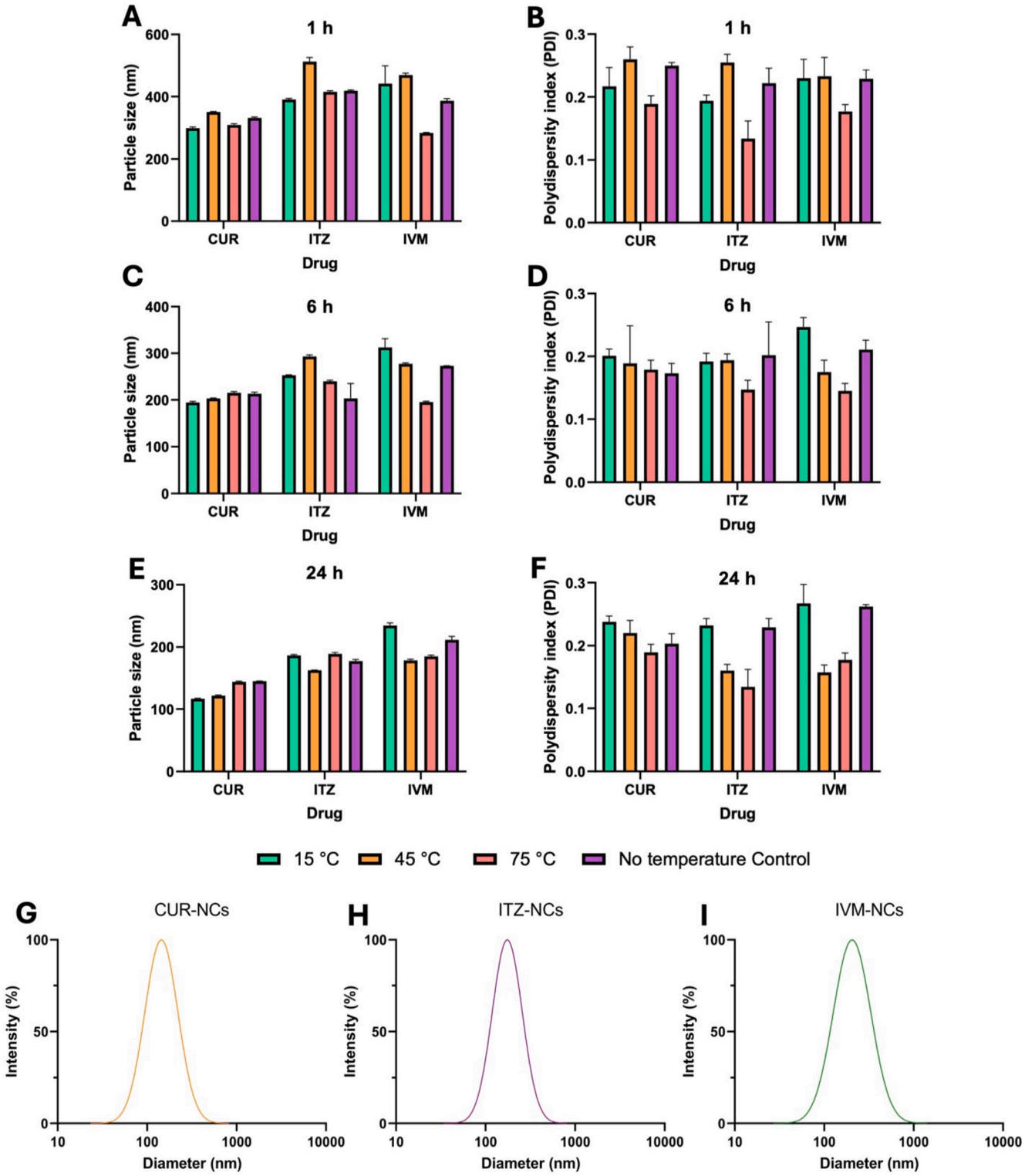

Fig. 4. Particle size and polydispersity index of CUR, ITZ and IVM nanosuspensions milled at various temperatures at 1 h- (**A, B**), 6 h- (**C, D**) and 24 h- (**E, F**) timepoints. Exemplar particle size distribution of CUR-NCs milled for 24 h at 15 °C (**G**), ITZ-NCs milled for 24 h at 45 °C (**H**), and IVM-NCs milled for 24 h at 45 °C (**I**).

structure, requiring increasing amounts of energy to break particles (Paredes et al., 2021). Thus, fine tuning of the temperature and milling time are crucial in early formulation development.

After 1 h of milling, the highest PDI values, in terms of CUR, were observed in both the vial maintained at 45 °C during milling and the non-temperature regulated vial (which attained a temperature of a similar level as presented in 3.2.), as depicted in Fig. 4**B**. This indicates an initial milling temperature of 45 °C negatively influences the particle size distribution of CUR, as the similarity of both PDI values, suggests both NSs were milled at comparable thermal conditions, resulting in corresponding patterns of particle breakage and distribution. This correlation highlights the important role of temperature during milling and its impact on the heterogeneity of particles produced during the milling process. However, after milling for 6 and 24 h, there was little variation

in the PDI observed between the milling of CUR at different temperatures, as indicated in Fig. 4. This shows the formulation is stable at all temperatures investigated and variation in temperature during later stages of milling has a less pronounced influence on the size of CUR particle populations produced. Interestingly, milling ITZ at 75 °C yielded a more favourable PDI with uniform particle sizes, producing a PDI<0.2, exhibiting a clear trend of manufacturing smaller PDI values, which is evidenced at all timepoints in Fig. 4**B, D and F**. It is plausible the reduced viscosity of milling slurry formed at higher temperatures, enabled enhanced movement and collision efficiency of the milling media, providing a uniform energy transfer leading to a more consistent particle size reduction which ultimately yields a homogenous PDI value. Unlike ITZ, IVM shows a change in trend, with milling at 75 °C initially providing a superior PDI value but with an extended period of milling for 24 h, a reduced temperature of 45 °C produced a more promising PDI value of 0.157 as opposed to that of 0.160 measured at 75 °C, as depicted in Fig. 4**F**. This change to a lower milling temperature for the production of a more favourable PDI, as milling time increases, is paralleled with respect to particle sizes, as displayed in Fig. 4. This may be attributed to the dynamic nature of particle size reduction, stabilisation processes and thermal effects, as milling IVM at high temperatures for short periods of time may be beneficial in terms of enhancing size reduction efficiency and preventing agglomeration. However, over longer milling periods, a lower milling temperature may be advantageous with respect to stabilising particles and preventing Ostwald ripening (Keck, 2010). A monomodal distribution of particle size for CUR-NCs (15 °C) ITZ-NCs (45 °C), and IVM-NCs (45 °C) is presented in Fig. 4**G**, **H** and **I**, respectively. From this data, it is evident that the Mini-mills could enable the development of optimal formulations enabling precise control of process variables at the laboratory-scale.

Temperature modification of the vial during milling demonstrated to affect the zeta potential of the NCs produced in a drug-dependent fashion, as detailed in Fig. 5. This is evident as all formulations were manufactured using the non-ionic surfactant POL188 comprised of sections of block copolymers polyethylene oxide (PEO) and polypropylene oxide (PPO) in a PEO-PPO-PEO formation (Bodratti and Alexandridis, 2018). Thus, POL188 is able to offer steric stabilisation as the hydrophilic polyethylene oxide chains coat the newly formed surfaces of the NCs, creating a hydrated layer providing steric hinderance, physically blocking close interaction with other particles and preventing aggregation (Verma et al., 2011). The zeta potentials for CUR, ITZ and IVM NCs at all temperatures indicated weaker electrostatic repulsion than the widely accepted range of $\geq |30|$ mV, probably due to low surface charges (Wang et al., 2013). This signifies a low level of electrostatic repulsion among drug nanoparticles, but it is not reflective of the steric stability provided by the physical barrier provided by POL188. As seen in Fig. 5, the variation in zeta potential is drug- and temperature-dependent. Importantly, the pH of all three NSs were close to neutral, (CUR: 6.48, ITZ:7.69 and IVM: 7.90). Although the drugs studied here are practically insoluble, particle size reduction to the nanometre range leads to a supersaturated state, and therefore, NCs coexist in equilibrium with soluble molecules (Mauludin et al., 2009). CUR presented an increasing trend in zeta potential values at increasing processing temperatures (Fig. 5**A**), which was attributed to changes on the adsorption/desorption of the stabiliser chains from the NCs' surface and induced charge effect. With pKa values of 8.38, 9.88 and 10.51, CUR exists primarily in its neutral form at the reported pH, and therefore, negligible effects on NCs' surface charge would be expected. The zeta potential of ITZ demonstrated similar values irrespective of the milling temperature, as evidenced in Fig. 5**B**, ranging between −4.5 to −8.0 mV. With a pKa

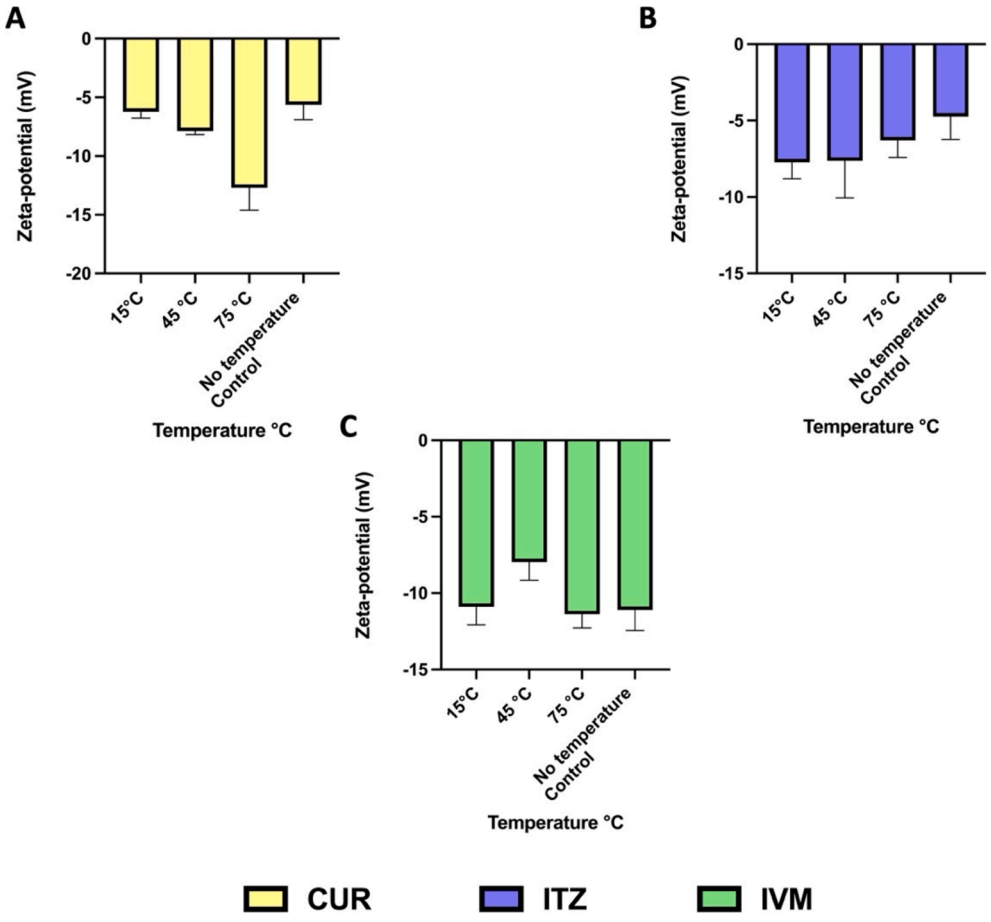

Fig. 5. Zeta potential of CUR (A), ITZ (B) and IVM (C) NSs milled for 24 h at 15 °C, 45 °C, 75 °C and without temperature control.

of 3.7, the drug is predominately in its neutral form at the reported pH, thus contributing minimally to the overall electrical charge of the NCs' surface. Similar trends were observed with IVM NSs (Fig. 5**C**), where working temperature showed a limited influence on the surface charge of the NCs, with all the produced suspensions presenting zeta potentials within |1.0| mV among them. At the reported pH, IVM, with a pKa of 12.47 would be mainly neutral, again with ionised IVM molecules contributing to the overall NCs surface charge minimally.

It can be observed that manipulation of temperature could be utilised as a key parameter to produce optimised NS as it is evident selection of temperature, for certain drugs, can vary the level of stabilisation of the newly formed particle surfaces. Thus, employment of the Mini-mills enables the exploration of stabilizers beyond the previously tested parameters by effective temperature management during milling.

3.3. Measurement of internal and external vial temperature during milling

The difference between the internal and external temperature of the vial was investigated as shown in Fig. 6. This was key to understand the ability of the circulating cooling liquid to absorb then heat created within the milling chamber. When using conventional glass vials with no temperature control, there was clear evidence of temperature raise. Initially, the external temperature of the non-temperature-controlled vial was 26.7 °C and the internal temperature was 25 °C, yet, as expected, a burst increase in temperature of 10 °C, both externally and internally, was observed during the first two hours of milling which then plateaued remaining elevated till the termination of milling at 24 h. This steep rise in temperature can be attributed to heat produced from the multitude of intense mechanical collisions between the drug, milling media, magnets and the glass vial (Afolabi et al., 2014). The heat generated during milling in the non-temperature-controlled vials is not effectively dissipated due to a lack of cooling mechanism leading to a sharp temperature increase of the vial internally and externally. This increase in temperature can influence the viscosity of the slurry, the overall process energy efficiency, and potentially the physical stability of the system via Ostwald ripening and affecting the adsorption and desorption of stabiliser molecules from the NCs' surface (Guner et al., 2022; Verma et al., 2011; Wang et al., 2013) Utilisation of the thermostat feedback system of the Ministat 125 (Huber, Offenburg, Germany) shown to be successful in precisely regulating the temperature of the vicious liquid circulating the temperature-controlled vials at three levels as the burst temperature increase was not observed at the set temperatures 15 °C, 45 °C and 75 °C. A slight disparity between the internal and external temperature was observed for the vials set at 45 °C and 75 °C, with the internal temperature of the vial remaining lower than the set values. A potential reason for the reduced temperature achieved includes the higher heat capacity of the NSs, than that of the glass of which the Mini-mills are composed of, which requires more energy to reach the desired temperature. Despite this slight limitation, it is important to note for all set temperatures evaluated, the measured temperatures remained consistent, highlighting a uniform temperature throughout the liquid was attained during the entirety of the milling process, as the feedback loop system of the Mini-mills remained effective over the 24-hour milling period measured.

3.4. Scanning electron microscopy (SEM) of coarse drugs and nanocrystals

In order to observe the change in surface morphology of the pure drugs as well as the different obtained NCs, the samples were examined using SEM. It can be seen in Fig. 7, the CUR presents particles apparently crystalline, with well-defined angular geometries, exhibiting rectangular and square shapes, with a relatively smooth and homogenous surface, with sizes in the range of ~ 20 to 120 μm. By contrast, the NCs obtained with the Mini- and NanoDisp® mills showed a significant change in appearance respect to the raw material, with the NCs embedded in a matrix of the dried stabiliser. This aligns with previous papers were NCs were dried by freeze or spray-drying (Paredes et al., 2020; Paredes et al., 2016). With respect to pure ITZ, a variety of irregularly shaped structures are observed, some angular in form with relatively smooth surfaces, consistent with the observations reported by other authors (Tao et al., 2009). The Mini-mill ITZ-NCs show clusters of smaller particles, whereas the scale-up ITZ-NCs are apparently more uniform. For IVM pure drug, particles of the drug can be observed in various shapes and sizes, with angular edges and rough surfaces. In both cases, the IVM-NCs formed *via* the Mini-mills and scale-up, a compact structure is observed. Noticeably, the IVM-NCs Mini-mills sample appears more uniform than the scale up sample, with some aggregates observed in the centre of the photomicrographs, probably formed during the drying process.

3.5. Microscopical analysis of YTZP zirconia beads after milling at different temperatures

YTZP yttria zirconia beads are engineered to withstand large amounts of energy, with application in various fields, including dyes manufacture, metallurgic, aerospace, and pharmaceutical industry. In this case, beads are engineered between 0.1–0.2 mm according to the manufacturer's specifications and changes of size and morphology were not expected. However, the beads before and after milling for 24 h at 75°C, presenting the more intense milling conditions, were analysed by SEM to confirm assess potential wearing, scratching or material loss. As observed in Fig. 8**A**, the beads with no use presented a near-perfect spherical shape and sizes according to the manufacturer specifications. The surface of the beads was smooth, and no noticeable defects were detected. Fig. 8**B, C, and D** correspond to the milling media collected from the production of CUR, ITZ, and IVM, respectively. Here, beads maintained their integrity during the milling process, as there was no

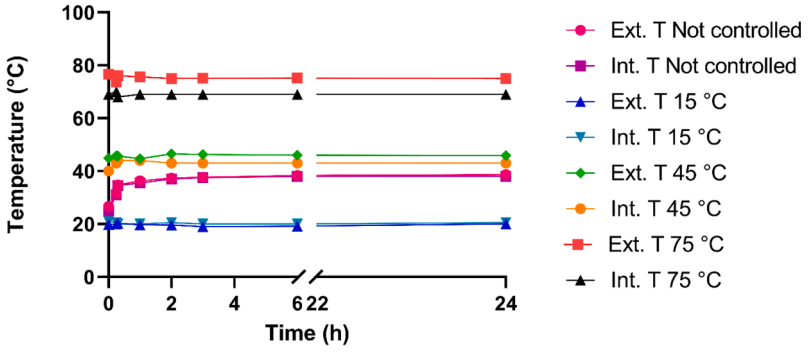

Fig. 6. Internal and external temperature of IVM formulation milled in novel temperature-controlled vials for 24 h at set temperatures of 15 °C, 45 °C, 75 °C and non-cooled vials at room temperature.

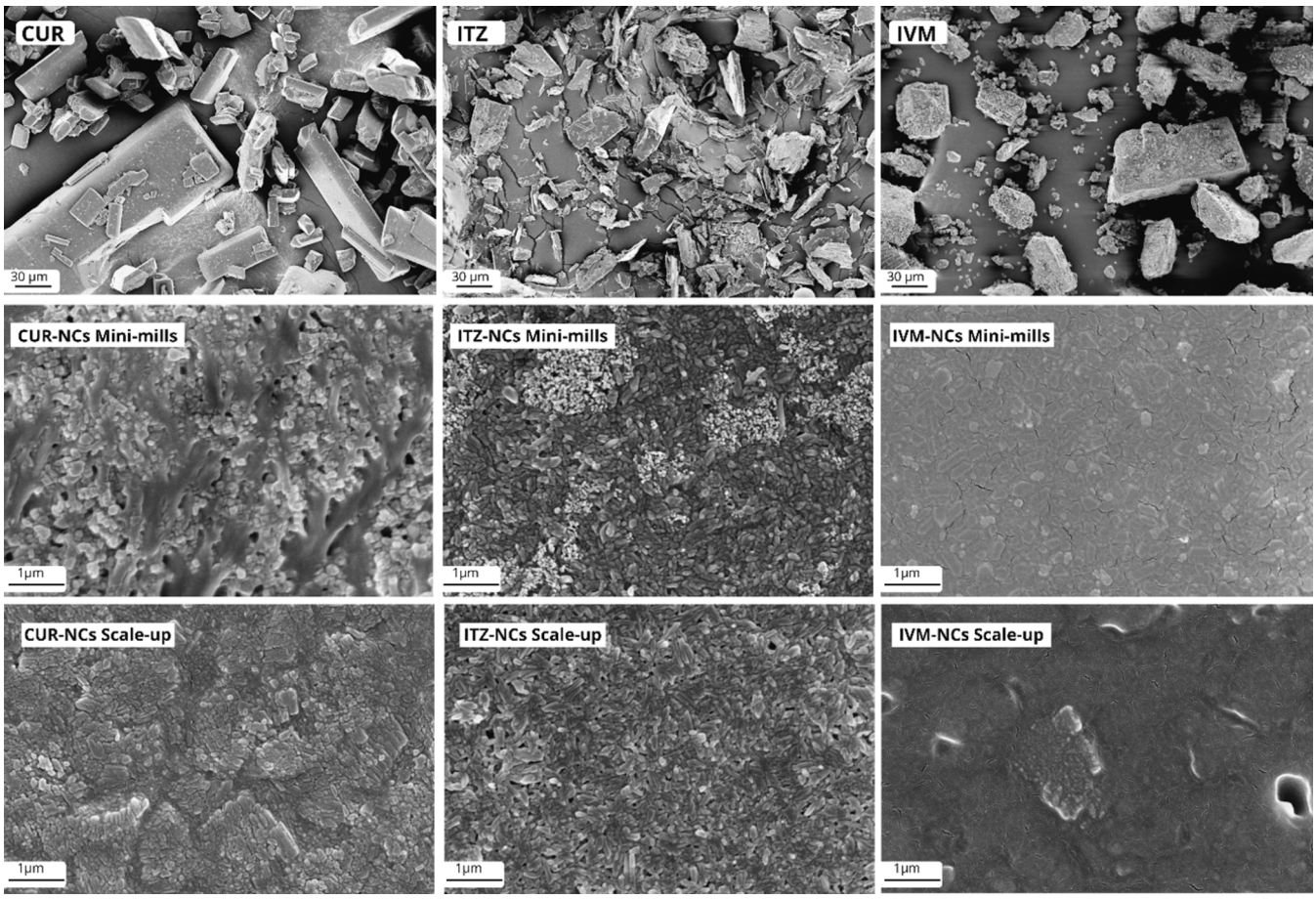

Fig. 7. SEM images of pure drugs, NCs produced in the Mini-mills and in the NanoDisp® media mill.

evidence of deformation or softening of the beads. Moreover, the surface of the beads post-milling was also smooth, with no apparent changes in size. This indicates that the milling media was able to withstand all collisions and shear forces, as well as the temperature and long processing time within the scope of this study. These findings are crucial since material transfer from the milling media to the resultant suspension is an important aspect of media milling (Juhnke et al., 2012). Importantly, industrial media mills can produce large batches of drug NSs under good manufacturing practices, reducing the chances of material wearing and contamination by coating all the mill parts (i.e., shaft and milling chamber) with the same ceramic materials of the milling media. Therefore, potential contamination in pre-clinical stages of NCs production can be remediated during formulation scale up.

3.6. Differential scanning calorimetry (DSC) and thermal gravimetric analysis (TGA)

The DSC and TGA thermograms of raw materials and freeze-dried NCs are reported in Fig. 9. The thermogram of CUR, Fig. 9**A**, showed an endothermic sharp peak at 185.6 °C, corresponding with the melting point of CUR (Boyd et al., 2019). ITZ showed a sharp endothermic peak at 168.8 °C in Fig. 9C which is coincident with the melting point of ITZ (Permana et al., 2020). In the case of IVM, two peaks were observed in the thermogram, the first peak was sharp and endothermic at 152.7 °C, corresponding with the melting point of the drug, while the second peak observed at 213.7 °C has associated mass loss, indicating thermal decomposition of the IVM as highlighted in Fig. 9**E** (Paredes et al., 2020). As shown in Fig. 9**A, C and E**, the thermal curve of POL188 exhibited a sharp endotherm with a temperature peak at 57.1 °C corresponding at melting point of the excipient used (Paredes et al., 2020). The DSC curve of CUR NCs showed two sharp and endothermic peaks at 51.4 °C and 154.6 °C corresponding with the melting point of POL188 and CUR. Similar thermal behaviour was observed for ITZ NCs. The DSC curve of Fig. 9**C** exhibited two sharp endothermic peaks at 51.4 °C and 163.8 °C, corresponding with the melting point of POL188 and ITZ, respectively. In the case of IVM NCs, the DSC curve showed only one event an endothermic peak at 51.4 °C corresponding with the melting point of POL188, while the melting point of IVM was detected in Fig. 9**E**. This behaviour can be attributed to the possibility of IVM dissolving in the molten POL188. The observed shifts to lower temperatures in the peak of each component in the NCs are related with the influence that particle size has in the thermal behaviour of crystalline components (Haddad et al., 2022). In this regard, smaller particles tend to exhibit lower melting points due to the increased surface area and enhanced surface energy associated with nanoscale materials. This phenomenon has been well documented in the literature for other poorly-soluble actives, where a similar shift to lower melting temperatures was observed as particle size decreased (Abbate et al., 2023; Zhang et al., 2023; Camiletti et al., 2020). Additionally, the interaction between the NCs and the stabilizing polymer further contributes to these thermal changes, as evidenced by Martin *et al.* (2020), showing a decrease in melting temperature when NCs are incorporated into a polymer matrix, suggesting a modification of intermolecular interactions between the particles and the polymer chains (Martin et al., 2020). For TGA, thermograms of CUR, ITZ, IVM, POL188 exhibit weight loss starting at approximately 240 °C, 350 °C, 145 °C and 330 °C respectively, indicating that the drugs and the stabilizer used are thermally stable up to each respective temperature as illustrated in Fig. 9**B, D and F**. TGA thermograms of CUR-NCs and ITZ-NCs, depicted in Fig. 9**B and D**, exhibited the beginning of mass loss at 240 °C and 350 °C showing that

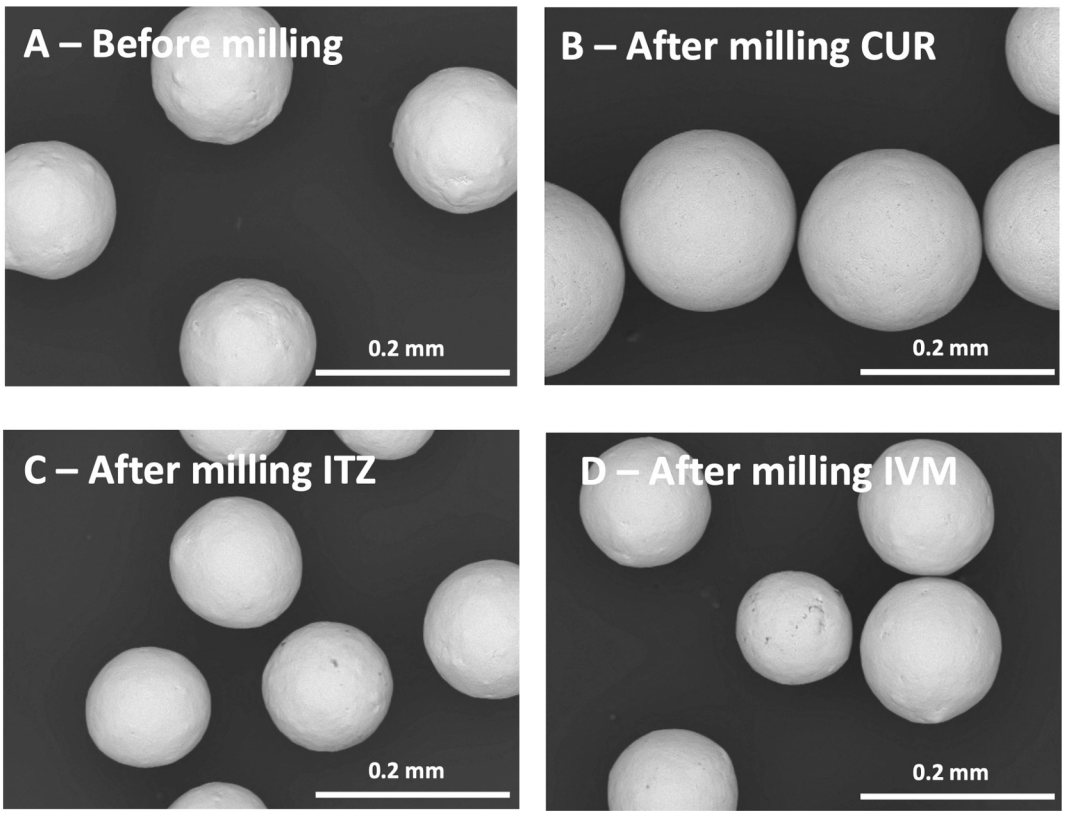

Fig. 8. SEM images of YTZP yttria zirconia beads before milling (**A**), and after milling CUR (**B**), ITZ (**C**), and IVM (**D**). Samples correspond to the 24 h time point and 75 °C, since they were the most energy-intensive milling conditions.

the NCs are thermally stable up to their respective temperatures, coincident behaviour to that of the pure drugs. IVM-NCs TGA thermogram showed mass loss initiated at 360 °C, indicating that IVM-NCs had similar thermal stable behaviour to POL188 (Fig. 9**F**). These results demonstrate that the process of NCs formation *via* media milling in the Mini-mill device does not interfere with the crystalline structure of each component used in the formulations as no polymorphic changes were observed on the process of NCs obtention. Thus, NCs composed of different active pharmaceutical ingredients can be successfully manufactured using the Mini-mill device.

3.7. Potential scale up of the Mini-mills

To evaluate the potential for scale-up of the Mini-mills, the NanoDisp® laboratory-scale mill (Cordoba, Argentina) was used (Paredes et al., 2020; Camiletti et al., 2020; Lopez-Vidal et al., 2021). This mill consists of an agitator chamber coupled to a variable-speed motor, where the milling material and the drug suspension are housed. In Fig. 10**A**, the particle size values for each evaluated drug are depicted over the course of milling time. It's evident that the particle size, as determined by DLS, decreases with the progression of milling. Following 1 h of milling, particle sizes of 473 ± 5 nm, 471 ± 9 nm, and 547 ± 10 nm are observed for CUR, ITZ, and IVM, respectively. Subsequently, after 4 h, both CUR and ITZ display values below 300 nm (264 ± 1 nm and 281 ± 4 nm, respectively), whereas IVM stands at 448 ± 4 nm. As discussed earlier, NCs typically exhibit a particle size ranging from 200-700 nm. In this regard, all three drugs studied showed sizes within the expected range and a tendency to decrease with milling time, suggesting that smaller sizes could be achieved by increasing the processing time if necessary. Regarding PDI, (Fig. 10**B**), acceptable values (<0.3) were achieved for all three drugs after 4 h of milling. These findings indicate that employing Mini-mills beforehand could optimize the formulation (including stabilizer selection and its compatibility with the drug, concentration of the original suspension, and the milling agent and its quantity) prior to transitioning to the laboratory-scale mill. This approach translates into substantial material savings, given that milling with NanoDisp® necessitates at least 12 times more drug compared to Mini-mills.

4. Conclusion

A novel method to successfully produce NCs at the milligram-scale in a temperature-controlled set up has been described in this report. When compared to other papers in the literature, the NCs produced using this simple experiment were small, with sizes as small as 116 nm in the case of CUR, showing substantial potential for the development of targeted systems, an area of increasing interest (Fuster et al., 2024; Udabe et al., 2024; Zhang et al., 2024). It was also demonstrated the applicability of the system to multiple actives, achieving homogeneous and monodisperse NSs in all cases, *via* precise control of temperature as a key variable for media milling of NCs. It was clear that particle size reduction and particle properties were highly dependent on the active, but in all cases, particle size reduction was achieved even after 1 h of milling. This is very appealing for optimisation of NCs using tools like design of experiment, which require a large number of milling iterations. Additionally, the use of this new method did not induce any substantial change in the drugs' crystallinity, as confirmed by DSC and TGA analysis. This study also demonstrated the potential for scale up to larger commercial mills, highlighting again the capabilities of a simple experimental approach that mimics processing conditions of larger scale mills. Employment of this milling method presents a flexible and simple technique for academic or industrial laboratories working in early development of drug NCs. Finally, this technique could also be translated to extraction of biological materials of interest from different tissues, cells and plants, all areas where thermal degradation could present significant challenges.

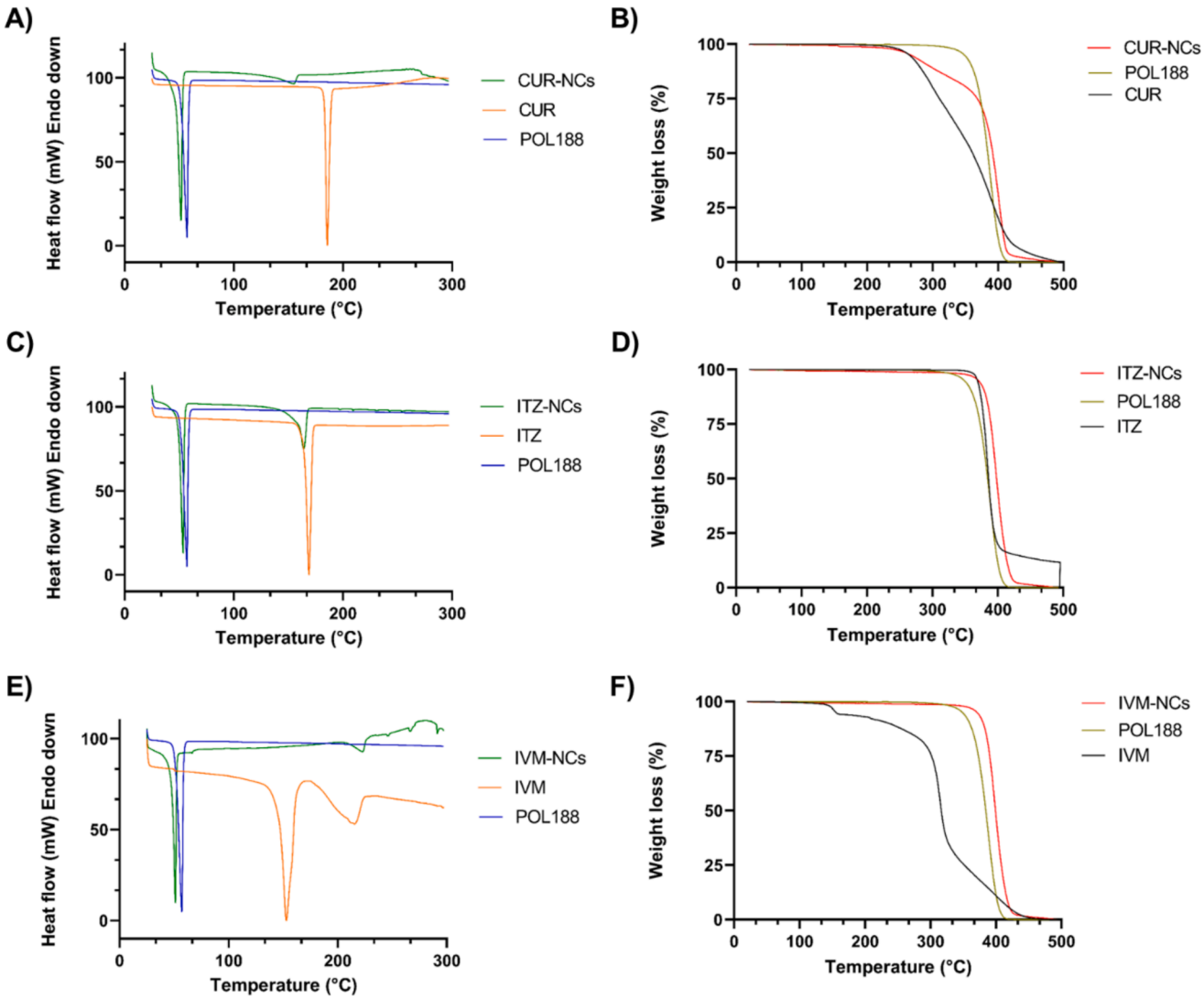

Fig. 9. Thermogravimetric analysis including DSC and TGA for CUR, ITZ and IVM and related samples.

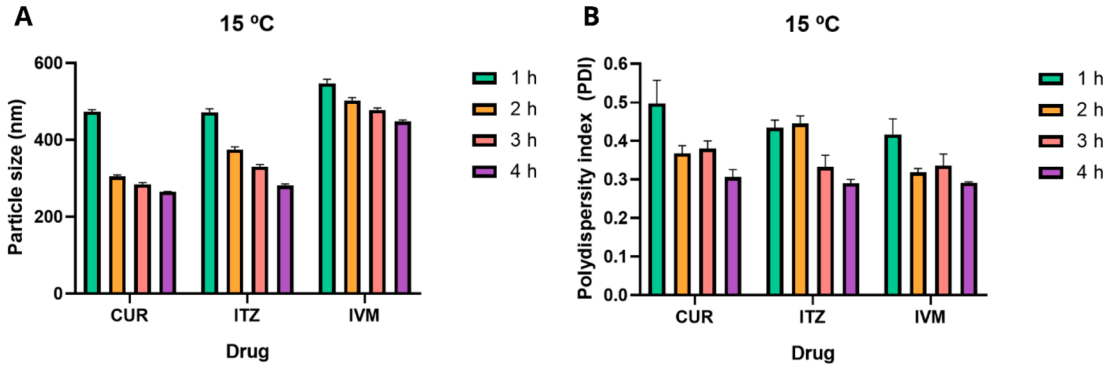

Fig. 10. Particle size (A) and PDI (B) of CUR, ITZ and IVM nanosuspensions milled at different milling times.

CRediT authorship contribution statement

Elise J. Catlin: Writing – original draft, Investigation, Data curation. **Octavio E. Fandino:** Writing – original draft, Investigation, Formal analysis, Data curation. **Lucía Lopez-Vidal:** Writing – original draft, Investigation, Data curation. **Martina Sangalli:** Investigation. **Ryan F. Donnelly:** Resources. **Santiago D. Palma:** Resources. **Alejandro J. Paredes:** Writing – review & editing, Writing – original draft, Supervision, Resources, Project administration, Methodology, Conceptualization.

Declaration of competing interest

The authors declare that they have no known competing financial

interests or personal relationships that could have appeared to influence the work reported in this paper.

Data availability

Data will be made available on request.

Acknowledgements

This work was supported by the Engineering and Physical Sciences Research Council (grant EP/Y001486/1), the Academy of Medical Sciences (SBF009\1019), and Applied Microbiology International *via* a New Lecturer Research Grant. The assistance from George Burton from the Glass Blowing Shop at Queen's University Belfast is much appreciated. E.J.C. holds a PhD studentship from Department of Economy of Northern Ireland. The authors thank the assistance from LAMARX Microscopy Centre for their assistance with SEM imaging. Additionally, gratitude is also expressed to Ms Gina Picco from @ggathmosphere visualization studio for the creation of the schematic Mini-mill images.

References

Abbate, M.T.A., Ramöller, I.K., Sabri, A.H., Paredes, A.J., Hutton, A.J., McKenna, P.E., Peng, K., Hollett, J.A., McCarthy, H.O., Donnelly, R.F., 2023. Formulation of antiretroviral nanocrystals and development into a microneedle delivery system for potential treatment of HIV-associated neurocognitive disorder (HAND). Int. J. Pharm., 123005 https://doi.org/10.1016/j.ijpharm.2023.123005.

Abbate, M.T.A., Ramöller, I.K., Sabri, A.H., Paredes, A.J., Hutton, A.J., McKenna, P.E., Peng, K., Hollett, J.A., McCarthy, H.O., Donnelly, R.F., 2023. Formulation of antiretroviral nanocrystals and development into a microneedle delivery system for potential treatment of HIV-associated neurocognitive disorder (HAND). Int. J. Pharm. 640, 123005. https://doi.org/10.1016/J.IJPHARM.2023.123005.

Afolabi, A., Akinlabi, O., Bilgili, E., 2014. Impact of process parameters on the breakage kinetics of poorly water-soluble drugs during wet stirred media milling: A microhydrodynamic view. Eur. J. Pharm. Sci. 51, 75–86. https://doi.org/10.1016/j.ejps.2013.09.002.

Bianchi, M.B., Zhang, C., Catlin, E., Sandri, G., Calderón, M., Larrañeta, E., Donnelly, R. F., Picchio, M.L., Paredes, A.J., 2022. Bioadhesive eutectogels supporting drug nanocrystals for long-acting delivery to mucosal tissues. Mater. Today Bio 17, 100471. https://doi.org/10.1016/J.MTBIO.2022.100471.

Bodratti, A.M., Alexandridis, P., 2018. Formulation of poloxamers for drug delivery. J. Funct. Biomater. 9. https://doi.org/10.3390/jfb9010011.

Boyd, B.J., Bergström, C.A.S., Vinarov, Z., Kuentz, M., Brouwers, J., Augustijns, P., Brandl, M., Bernkop-Schnürch, A., Shrestha, N., Préat, V., Müllertz, A., Bauer-Brandl, A., Jannin, V., 2019. Successful oral delivery of poorly water-soluble drugs both depends on the intraluminal behavior of drugs and of appropriate advanced drug delivery systems. Eur. J. Pharm. Sci. 137, 104967. https://doi.org/10.1016/J.EJPS.2019.104967.

Camiletti, B.X., Camacho, N.M., Paredes, A.J., Allemandi, D.A., Palma, S.D., Grosso, N., 2020. Self-dispersible nanocrystals of azoxystrobin and cyproconazole with increased efficacy against soilborne fungal pathogens isolated from peanut crops. Powder Technol. 372, 455–465. https://doi.org/10.1016/j.powtec.2020.06.025.

Castillo Henríquez, L., Bahloul, B., Alhareth, K., Oyoun, F., Frejková, M., Kostka, L., Etrych, T., Kalshoven, L., Guillaume, A., Mignet, N., Corvis, Y., 2024. Step-by-step standardization of the bottom-up semi-automated nanocrystallization of pharmaceuticals: A quality by design and design of experiments joint approach. Small 20. https://doi.org/10.1002/smll.202306054.

Chen, H., Khemtong, C., Yang, X., Chang, X., Gao, J., 2011. Nanonization strategies for poorly water-soluble drugs. Drug Discov. Today 16, 354–360. https://doi.org/10.1016/J.DRUDIS.2010.02.009.

Dahan, A., Beig, A., Lindley, D., Miller, J.M., 2016. The solubility–permeability interplay and oral drug formulation design: Two heads are better than one. Adv. Drug Deliv. Rev. 101, 99–107. https://doi.org/10.1016/J.ADDR.2016.04.018.

S.M. Dizaj, Z. Vazifehasl, S. Salatin, K. Adibkia, Y. Javadzadeh, Nanosizing of drugs: Effect on dissolution rate, 2015.

Fuster, M.G., Wang, J., Fandiño, O., Víllora, G., Paredes, A.J., 2024. Folic acid-decorated nanocrystals as highly loaded trojan horses to target cancer cells. Mol. Pharm. 21, 2781–2794. https://doi.org/10.1021/acs.molpharmaceut.3c01186.

Guner, G., Yilmaz, D., Yao, H.F., Clancy, D.J., Bilgili, E., 2022. Predicting the temperature evolution during nanomilling of drug suspensions via a semi-theoretical lumped-parameter model. Pharmaceutics 14, 2840. https://doi.org/10.3390/pharmaceutics14122840.

Guner, G., Seetharaman, N., Elashri, S., Mehaj, M., Bilgili, E., 2022. Analysis of heat generation during the production of drug nanosuspensions in a wet stirred media mill. Int. J. Pharm. 624, 122020. https://doi.org/10.1016/j.ijpharm.2022.122020.

Haddad, R., Alrabadi, N., Altaani, B., Li, T., 2022. Paclitaxel drug delivery systems: focus on nanocrystals' surface modifications. Polymers (Basel) 14. https://doi.org/10.3390/polym14040658.

Juhnke, M., Märtin, D., John, E., 2012. Generation of wear during the production of drug nanosuspensions by wet media milling. Eur. J. Pharm. Biopharm. 81, 214–222. https://doi.org/10.1016/j.ejpb.2012.01.005.

Junyaprasert, V.B., Morakul, B., 2015. Nanocrystals for enhancement of oral bioavailability of poorly water-soluble drugs. Asian J. Pharm. Sci. 10, 13–23. https://doi.org/10.1016/J.AJPS.2014.08.005.

Keck, C.M., 2010. Particle size analysis of nanocrystals: Improved analysis method. Int. J. Pharm. 390, 3–12. https://doi.org/10.1016/j.ijpharm.2009.08.042.

Lipinski, C., 2002. Poor aqueous solubility-an industry wide problem in ADME screening. Am. Pharm. Rev. 5, 82–85.

Liversidge, G.G., Cundy, K.C., 1995. Particle size reduction for improvement of oral bioavailability of hydrophobic drugs: I. Absolute oral bioavailability of nanocrystalline danazol in beagle dogs. Int. J. Pharm. 125, 91–97. https://doi.org/10.1016/0378-5173(95)00122-Y.

Lopez-Vidal, L., Pablo Real, J., Andrés Real, D., Camacho, N., Kogan, M.J., Paredes, A.J., Daniel Palma, S., 2021. Nanocrystal-based 3D-printed tablets: Semi-solid extrusion using melting solidification printing process (MESO-PP) for oral administration of poorly soluble drugs. Int. J. Pharm., 121311 https://doi.org/10.1016/j.ijpharm.2021.121311.

Ma, P., Seguin, J., Ly, N.K., Henríquez, L.C., Plansart, E., Hammad, K., Gahoual, R., Dhôtel, H., Izabelle, C., Saubamea, B., Richard, C., Escriou, V., Mignet, N., Corvis, Y., 2022. Designing fisetin nanocrystals for enhanced in cellulo anti-angiogenic and anticancer efficacy. Int. J. Pharm. X 4, 100138. https://doi.org/10.1016/J.IJPX.2022.100138.

Malamatari, M., Taylor, K.M.G., Malamataris, S., Douroumis, D., Kachrimanis, K., 2018. Pharmaceutical nanocrystals: Production by wet milling and applications. Drug Discov. Today 23, 534–547. https://doi.org/10.1016/J.DRUDIS.2018.01.016.

B. Martin, J. Seguin, M. Annereau, T. Fleury, R. Lai-Kuen, G. Neri, A. Lam, M. Bally, N. Mignet, Y. Corvis, Preparation of parenteral nanocrystal suspensions of etoposide from the excipient free dry state of the drug to enhance in vivo antitumoral properties, Scientific Reports 2020 10:1 10 (2020) 1–13. Doi: 10.1038/s41598-020-74809-z.

Mauludin, R., Müller, R.H., Keck, C.M., 2009. Development of an oral rutin nanocrystal formulation. Int. J. Pharm. 370, 202–209. https://doi.org/10.1016/j.ijpharm.2008.11.029.

McGuckin, M.B., Wang, J., Ghanma, R., Qin, N., Palma, S.D., Donnelly, R.F., Paredes, A. J., 2022. Nanocrystals as a master key to deliver hydrophobic drugs via multiple administration routes. J. Control. Release 345, 334–353. https://doi.org/10.1016/j.jconrel.2022.03.012.

R.H. Müller, R. Shegokar, S. Gohla, C.M. Keck, Nanocrystals: Production, Cellular Drug Delivery, Current and Future Products, in: A. Prokop (Ed.), Intracellular Delivery: Fundamentals and Applications, Springer Netherlands, Dordrecht, 2011: pp. 411–432. Doi: 10.1007/978-94-007-1248-5_15.

Muller, R.H., Keck, C.M., 2004. Challenges and solutions for the delivery of biotech drugs – A review of drug nanocrystal technology and lipid nanoparticles. J. Biotechnol. 113, 151–170. https://doi.org/10.1016/j.jbiotec.2004.06.007.

Niwa, T., Nakanishi, Y., Danjo, K., 2010. One-step preparation of pharmaceutical nanocrystals using ultra cryo-milling technique in liquid nitrogen. Eur. J. Pharm. Sci. 41, 78–85. https://doi.org/10.1016/j.ejps.2010.05.019.

Noyes, A.A., Whitney, W.R., 1897. The rate of solution of solid substances in their own solutions. J. Am. Chem. Soc. 19, 930–934. https://doi.org/10.1021/ja02086a003.

A.J. Paredes, N.M. Camacho, L. Schofs, A. Dib, M. del P. Zarazaga, N. Litterio, D.A. Allemandi, S. Sánchez Bruni, C. Lanusse, S.D. Palma, Ricobendazole nanocrystals obtained by media milling and spray drying: Pharmacokinetic comparison with the micronized form of the drug, Int J Pharm 585 (2020) 119501. Doi: 10.1016/J.IJPHARM.2020.119501.

Paredes, A.J., Llabot, J.M., Sánchez Bruni, S., Allemandi, D., Palma, S.D., 2016. Self-dispersible nanocrystals of albendazole produced by high pressure homogenization and spray-drying. Drug Dev. Ind. Pharm. 42, 1564–1570. https://doi.org/10.3109/03639045.2016.1151036.

Paredes, A.J., McKenna, P.E., Ramöller, I.K., Naser, Y.A., Volpe-Zanutto, F., Li, M., Abbate, M.T.A., Zhao, L., Zhang, C., Abu-Ershaid, J.M., Dai, X., Donnelly, R.F., 2021. Microarray patches: Poking a hole in the challenges faced when eelivering poorly soluble drugs. Adv. Funct. Mater. 31. https://doi.org/10.1002/adfm.202005792.

Peltonen, L., 2018. Design space and QbD approach for production of drug nanocrystals by wet media milling techniques. Pharmaceutics 10. https://doi.org/10.3390/pharmaceutics10030104.

Permana, A.D., Paredes, A.J., Volpe-Zanutto, F., Anjani, Q.K., Utomo, E., Donnelly, R.F., 2020. Dissolving microneedle-mediated dermal delivery of itraconazole nanocrystals for improved treatment of cutaneous candidiasis. Eur. J. Pharm. Biopharm. 154, 50–61. https://doi.org/10.1016/J.EJPB.2020.06.025.

Permana, A.D., Paredes, A.J., Zanutto, F.V., Muh, N., Amir, I.I., Muh, A., Bahar, S., Palma, S.D., Donnelly, R.F., 2021. Albendazole nanocrystal-based dissolving microneedles with improved pharmacokinetic performance for enhanced treatment of cystic echinococcosis. ACS Appl. Mater. Interfaces 13, 38745–38760. https://doi.org/10.1021/acsami.1c11179.

Romero, G.B., Keck, C.M., Müller, R.H., 2016. Simple low-cost miniaturization approach for pharmaceutical nanocrystals production. Int. J. Pharm. 501, 236–244. https://doi.org/10.1016/J.IJPHARM.2015.11.047.

Tao, T., Zhao, Y., Wu, J., Zhou, B., 2009. Preparation and evaluation of itraconazole dihydrochloride for the solubility and dissolution rate enhancement. Int. J. Pharm. 367, 109–114. https://doi.org/10.1016/j.ijpharm.2008.09.034.

Udabe, J., Martin-Saldaña, S., Tao, Y., Picchio, M., Beloqui, A., Paredes, A.J., Calderón, M., 2024. Unveiling the potential of surface polymerized drug nanocrystals in targeted delivery. ACS Appl. Mater. Interfaces. https://doi.org/10.1021/acsami.4c07669.

J. -Uwe, A.H. Junghanns, R.H. Müller, Nanocrystal technology, drug delivery and clinical applications, 2008.
Verma, S., Kumar, S., Gokhale, R., Burgess, D.J., 2011. Physical stability of nanosuspensions: Investigation of the role of stabilizers on Ostwald ripening. Int. J. Pharm. 406, 145–152. https://doi.org/10.1016/j.ijpharm.2010.12.027.
Wang, Y., Zheng, Y., Zhang, L., Wang, Q., Zhang, D., 2013. Stability of nanosuspensions in drug delivery. J. Control. Release 172, 1126–1141. https://doi.org/10.1016/j.jconrel.2013.08.006.
Wu, Y., Vora, L.K., Mishra, D., Adrianto, M.F., Gade, S., Paredes, A.J., Donnelly, R.F., Singh, T.R.R., 2022. Nanosuspension-loaded dissolving bilayer microneedles for hydrophobic drug delivery to the posterior segment of the eye. Biomater. Adv. 137, 212767. https://doi.org/10.1016/J.BIOADV.2022.212767.
Zhang, C., Jahan, S.A., Zhang, J., Bianchi, M.B., Volpe-Zanutto, F., Baviskar, S.M., Rodriguez-Abetxuko, A., Mishra, D., Magee, E., Gilmore, B.F., Singh, T.R.R., Donnelly, R.F., Larrañeta, E., Paredes, A.J., 2023. Curcumin nanocrystals-in-nanofibres as a promising platform for the management of periodontal disease. Int. J. Pharm. 648, 123585. https://doi.org/10.1016/J.IJPHARM.2023.123585.
Zhang, C., Vora, L.K., Tekko, I.A., Volpe-Zanutto, F., Peng, K., Paredes, A.J., McCarthy, H.O., Donnelly, R.F., 2023. Development of dissolving microneedles for intradermal delivery of the long-acting antiretroviral drug bictegravir. Int. J. Pharm. 642, 123108. https://doi.org/10.1016/j.ijpharm.2023.123108.
Zhang, C., Lopez-Vidal, L., Wang, J., Himawan, A., Donnelly, R.F., Paredes, A.J., 2024. Mucoadhesive itraconazole nanocrystals with precise control of surface charge incorporated to chitosan films for buccal drug delivery. Adv. Ther. (Weinh). https://doi.org/10.1002/adtp.202400209.